Use of graphite oxide and/or thermally reduced graphite oxide for the removal of dyes from water

Use of graphite oxide and/or thermally reduced graphite oxide for the removal of dyes from water

P. Avetta[a], M. Sangermano[b], M. Lopez-Manchado[c], P. Calza[a,*]

[a] Università di Torino, Dipartimento di Chimica, via P. Giuria 5, 10125 Torino, Italy

[b] Dipartimento di Scienza Applicata e Tecnologia, Politecnico di Torino, C.so Duca degli Abruzzi 24, 10129 Torino, Italy

[c] Instituto de Ciencia y Tecnologia de Polimeros, ICTP-CSIC, Juan de la Cierva, 3, 28006 Madrid, Spain

*corresponding author

e-mail: paola.calza@unito.it; phone: +390116705268; fax: +390116705242

Abstract

Two types of carbonaceous materials, graphite oxide (GOx) and thermally reduced graphite oxide (TRGO) were tested in the dyes removal from water. Two common synthetic aquatic pollutants, Orange II, an azo dye, and Rhodamine B, a xanthene dye, were selected as probe molecules and their bleaching was evaluated.

We observed that the two materials act in a different way when dispersed in aqueous solution: TRGO acts as a good adsorbent material whereas GOx can be used as an efficient photosensitizer.

Dye removal is almost complete in the dark in the presence of TRGO and within few minutes a steady-state concentration was achieved. On the contrary, in the case of GOx, adsorption is limited to almost 10%-20% for both dyes, but this material is able to induce dyes photodegradation and almost 80% of the residual dyes are abated within 5 hours of irradiation under simulated solar light. When the graphene derivatives were dispersed in UV-cured acrylic polymeric films, the reduction of the surface area dropped the adsorption properties of TRGO, whereas the photosensitizer properties of GOx were maintained and the bleaching of the two dyes was achieved.

Keywords: graphite oxide, thermally reduced graphite oxide, dyes, UV-curing, solar light

1. INTRODUCTION

Dyes are among common synthetic aquatic pollutants of possible environmental concern, because of their extensive, widespread use. These compounds are quite difficult to remove from water since they are resistant to light and oxidizing agents. Their presence in wastewaters has to be carefully considered, as not even biological degradation was effective in their elimination, the efficiency largely depending on the dye structure. Biodegradation of dyes is in general not efficient enough, due to the presence of complex and stable aromatic structures. For these reasons, the most common approach for water treatment involves the use of Advanced Oxidation Processes in order to obtain the complete abatement of dyes and possibly the mineralization of the organic carbon. Among these technologies, TiO_2 mediated photocatalysis has been demonstrated to be efficient in decolorize dye effluent in the presence of UV–Visible light. Many papers in the last years dealt in particularly with the TiO_2 assisted degradation of anthraquinone, quinoline and azo dyes [1-8], showing good results in both dye bleaching and mineralization.

The use of graphene was recently proposed by several groups for the preparation of highly photoactive composite materials based on titanium dioxide for the catalytic oxidation of organic pollutants in aqueous solutions [9-12], in order to exploit the high charge mobility of graphene and to maximize the photocatalytic efficiency by hindering the process of charge recombination. Furthermore, it is well known that the band-gap of graphene derivatives, and therefore their photosensitizer properties, can be tuned by modifying the degree of oxidation, with a change of the optical gap from 3.5 eV down to 1 eV by increasing the C/O ratio. Likewise, the ability of graphite oxide (GOx) to act as photosensitizer when dispersed in aqueous solution or dispersed in a polymeric film has been very recently proved [13,14].

An alternative method to remove pollutants from water is the adsorption process, which has been proved to be reliable for dye treatment [15,16]; several materials, i.e. silica aerogels [17], chitosan [18] and graphene [19] have been proposed as efficient absorbent materials for dye removal from water. Concerning graphene, the interaction between the contaminant and the adsorbent material can be controlled by several mechanisms, including electrostatic attraction and π-π stacking. Conversely, when employing graphite oxide as adsorbant material, surficial charge has also to be considering. In fact, the presence of surficial adsorption capacity is strongly linked to the presence of surficial negatively charged groups, that are able to promote the adsorption of cationic pollutants [20-22], but may hinder the adsorption of anionic pollutants.

Taking into account the above reported literature and our previous experience in this field, we have investigated the role played by graphite oxide (GOx) and thermally reduced graphite oxide (TRGO)

in the removal from water of an anionic dye, Orange II, and a xanthene dye, Rhodamine B, holding both positively and negatively charged moieties. We try to exploit the key peculiarities of these materials to obtain materials tunable in the way of action combining the photoactivity of GOx, that shows a typical band-gap of semiconductor, and the high adsorption capability of TRGO. Furthermore we present here for the first time the possibility to use them not only dispersed in aqueous solution but also within a polymeric coating.

2. EXPERIMENTAL

2.1. Materials

Orange II (OII) and Rhodamine B (RB) were purchased from Aldrich. Thermally reduced graphite oxide (TRGO) were synthesized by the reduction and thermal exfoliation of graphite oxide at 1000 °C for 30 sec. Graphite oxide (GOx) was previously obtained using natural graphite flakes (purum powder B0.1 mm, Sigma-Aldrich) following the Brodie method. GOx produced through this method leads to the formation of single graphene layers or stacks of up to seven sheets with hydroxyl, carbonyl, and epoxy groups on their surface [23]. A full description of the synthesis and characterization of the thermally reduced graphite oxide (TRGO) can be found elsewhere [24].

The acrylic resin polyethyleneglycol diacrylate (PEGDA, Aldrich, Mw ≈ 740 g/mol, density = 1.12 g/cm^3) was used to prepare the crosslinked films in the presence of 2 wt% of the photoinitiator 2-hydroxy-2-methyl-1-phenyl-propan-1-one (Darocur® 1173, BASF®) with respect to the acrylic resin in order to promote the UV-curing process.

All aqueous solutions were prepared with ultrapure water (Millipore MilliQ^{TM}).

2.2. Material characterization

Raman spectroscopy was performed on a Renishaw Invia Raman Microscope, using an argon laser with at 514.5 nm excitation wavelength. The carbon nanoparticles were placed on a glass slide and air-dried before the measurements were taken. This technique allows analyzing the structural quality of graphitic materials since the amount of ordering and degree of sp^2 and sp^3 bonding provides a unique Raman "fingerprint" for each carbon structure.

The morphology of the graphene was observed using a Philips XL30 environmental scanning electron microscopy (ESEM) at 15 kV and by transmission electron microscopy (TEM). TEM images were obtained with a Jeol JEM 2100 TEM apparatus using an accelerating voltage of 200

kV. The samples were prepared by drop-casting a dilute suspension in THF onto a carbon grid and allowing the solvent to evaporate.

2.3. Investigation using dispersions in aqueous solution

For the photocatalysis experiments, the dyes were irradiated under continuous stirring in the presence of carbonaceous materials (5 mL total volume) in closed Pyrex® cells with a Xenon lamp (1500W, Solarbox) equipped with a 400 nm cut-off filter. For the adsorption investigation the dyes were put in contact in the dark, under continuous stirring, with the adsorbent materials.

The dyes bleaching at different irradiation time (for the photocatalysis) and at different contact time (for the adsorption), were followed by means of Varian CARY 100 Scan UV-Vis spectrophotometer using Suprasil quartz cuvettes with a path length of 1 cm. The spectrophotometric determination was done at 552 nm for RB and at 486 nm for OII.

2.4. Investigation using PEGDA films

For dyes removal study using PEGDA-UV cured films, the carbonaceous filler was added to the epoxy resin in order to prepare hybrid materials with different percentages of GOx and/or TRGO respect to the epoxy resin. The mixtures were stirred with Ultraturrex until a uniform dispersion was achieved. The photoinitiator was added at 2 wt% in each formulations, coated on glass substrate and UV irradiated under nitrogen atmosphere, by means of a UV-lamp, with a light intensity on the surface of the sample of about 30 mW/cm^2. Free-standing UV cured films of about 100 μm were achieved. The kinetics of the photopolymerization was determined, both for the pristine and filled formulations, by real time FT-IR spectroscopy employing a Thermo-Nicolet 5700 instrument. The liquid formulations were coated onto a silicon wafer with a thickness of 50 μm and exposed simultaneously to the UV light (medium pressure mercury lamp Hamamatsu LC8, light intensity on the surface of the sample of about 30 mW/cm^2), which induces the polymerization, and to the IR beam, which analyzes *in situ* the extent of the reaction. Acrylic double bond conversion was followed by monitoring the decrease in the absorbance due to acrylic double bonds centered at around 1640 cm^{-1}. The gel content of UV-cured acrylic films was determined by measuring the weight loss after 24 hours extraction with chloroform at room temperature, according to the standard test method ASTM D2765-84. DSC measurements were performed on cured films under nitrogen flux, in the range between -120 °C to 80 °C, with a DSCQ 1000 of TA Instruments equipped with a low temperature probe.

The acrylic crosslinked films were immersed into the dyes aqueous solutions and the color disappearance was analyzed, at different times, by means of UV–Vis spectrophotometer as previously described.

3. RESULTS AND DISCUSSION

3.1. Material characterization

The XRD and XPS analysis were already published [24, 25], where the authors named TRGO as functionalized graphite sheets (FGS) and GOx as GO; hereafter, a brief discussion concerning these results follows.

XRD measurements show that natural graphite presents a diffraction maximum at 2θ=26° corresponding to an interlayer spacing d=0.34 nm. After the oxidation process, the value of the natural graphite (NG) diffraction maximum decreases to 2θ =17° (d=0.52 nm) due to the intercalation of oxygen groups on the basal plane. After the thermal reduction of GOx, TRGO presents a broad and weak maximum around 2θ=24° indicating that most of the TRGO material consists on exfoliated graphite [24].

XPS was employed to analyse the nature and the relative amount of oxygen containing functional groups present on the graphene surface. The C_{1s} spectra can be deconvoluted in 4 symmetrical components. That is, the main intense peak at 284.8 eV is assigned to sp^2 and sp^3 carbon atoms, while the peaks on the region 286.3-286.5 eV and 288.0-289.0 eV correspond to C-O-C and O-C=O functional groups, respectively. It is worth noting that the peak corresponding to the signature of graphitic carbon (291.0-291.5 eV) is still present in the TRGO sample. This peak is known as the shake-up satellite of the 284.8 eV and it is characteristic of graphitic systems, which means that the exfoliation process at high temperatures is able to restore the graphitic structure. Although the C_{1s} spectrum provides information about the plausible functional groups on TRGO, the O_{1s} spectrum complements the later. Thus, the deconvolution of O_{1s} spectrum resulted in two main peaks: one at 531.5 eV which corresponds to O=C-O groups and other at 533.7 eV, which is assigned to C-O-C groups [25].

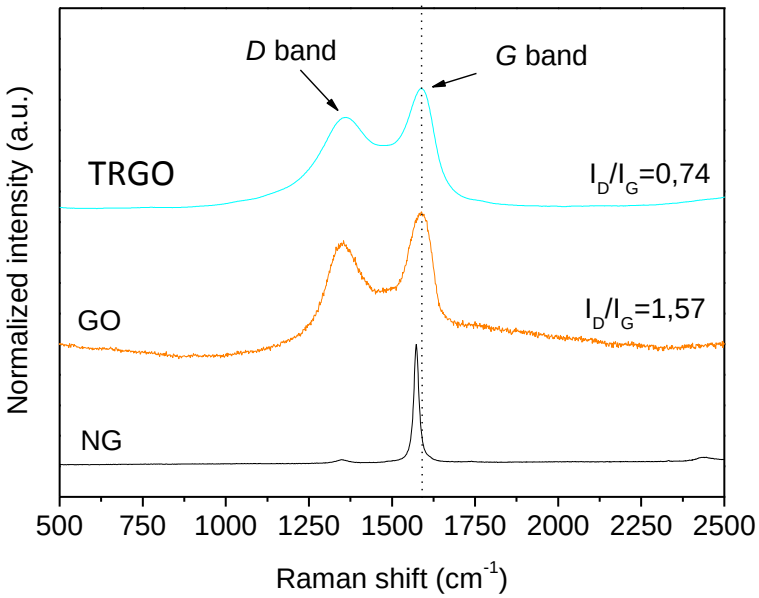

Figure 1. Raman spectra of the synthesis path: natural graphite (NG), graphite oxide (GOx) and thermally reduced graphite oxide (TRGO).

The significant structural changes occurring during the oxidation-reduction processing from NG to GOx, and then to TRGO, are reflected in their Raman spectra which are shown in Figure 1.

The Raman spectrum of the pristine graphite displays a prominent *G* peak as the only feature at 1573 cm^{-1}, corresponding to the first-order scattering of the E_{2g} phonon mode of sp^2 C atoms. Specifically, from NG to GOx, the *G* band is broadened significantly and displays a shift to higher Raman shift (from 1573 cm^{-1} to 1588 cm^{-1}) since GOx exhibit higher disorder than NG as a result of the oxidation process. In addition, the appearance of a prominent *D* band at 1348 cm^{-1} indicates the reduction in size of the in-plane sp^2 domains, possibly due to the extensive oxidation process. Raman spectrum of the TRGO also contains both *D* and *G* bands (1361 and 1588 cm^{-1}, respectively), with a decreased I_D/I_G intensity ratio compared to GOx which is attributed to a "self-healing" behaviour during the thermal expansion [26] and the re-structuration of the aromatic structure.

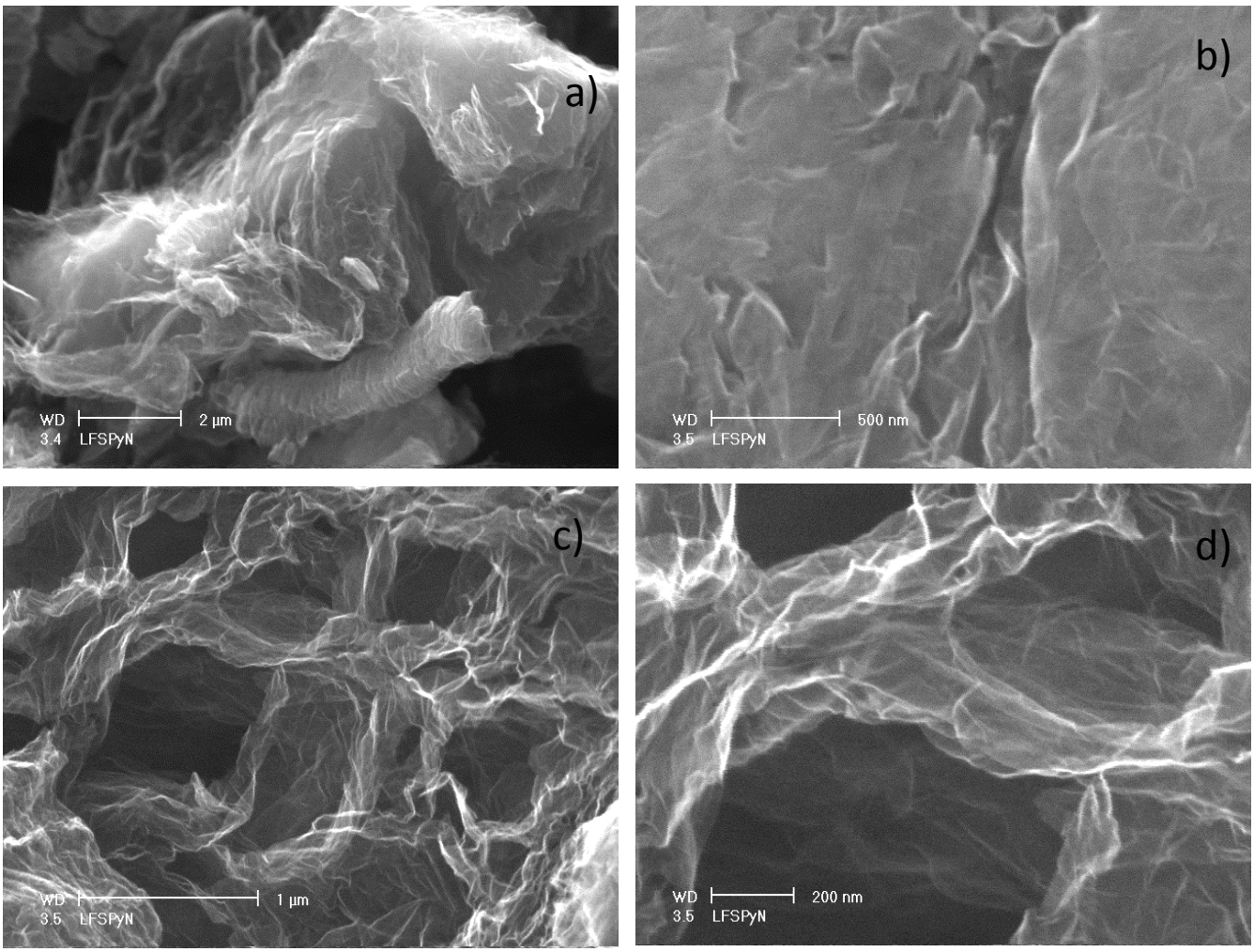

Figure 2. SEM images of thermally reduced graphite oxide (TRGO)

Scanning and transmission electron microscopy images (Figure 2 and 3) revealed that the functionalized graphene sheets are formed by randomly aggregated and very thin crumpled sheets.

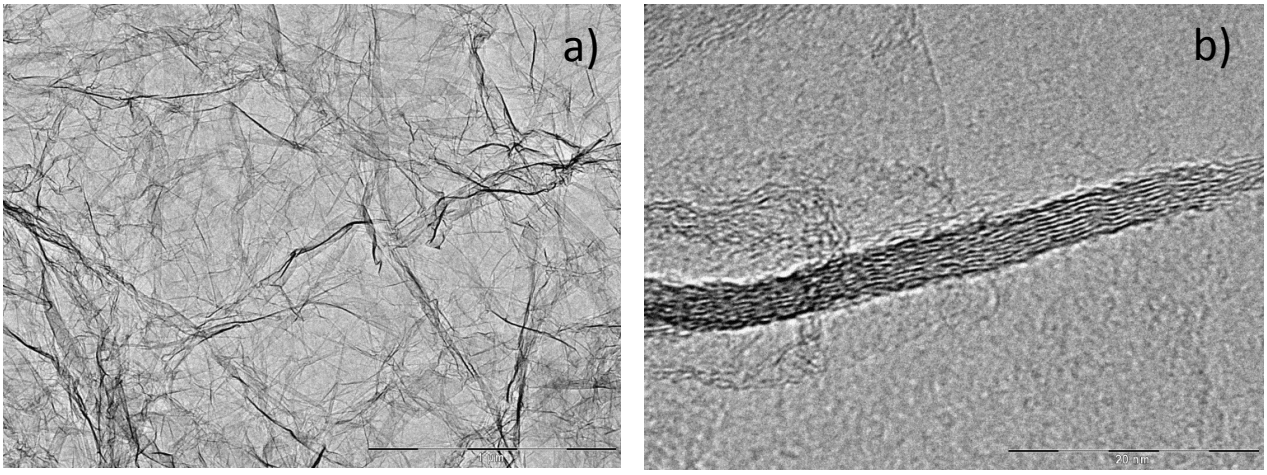

Figure 3. TEM images of thermally reduced graphite oxide (TRGO)

TEM images (Figure 3) also show the characteristic wrinkled structure of the particle due to the thermal shock to which it has been subjected. TRGO are composed of approximately 5-6 individual sheets with an interlayer distance about 0.6 nm, thus corroborating the XRD results.

3.2. Removal of dyes

OII and RB were used as probe molecules to evaluate both the adsorption in the dark and the photoactivity of carbon nanoparticles (CNPs). At first the carbonaceous materials were dispersed in water and the dyes adsorption and photodegradation were evaluated over time. Secondly, these materials were dispersed within a UV-cured polymeric film and the occurrence of adsorption and photodegradation processes were investigated.

3.2.1. Carbonaceous materials dispersed in aqueous solution

Adsorption in the dark of OII and RB with both CNPs was performed. In all cases, adsorption rapidly occurred and within few seconds a steady-state concentration was achieved (data not shown). Table 1 collects all data obtained with TRGO and GOx adsorption process is particularly important when employing TRGO toward RB that is almost completely removed within 1 minute. Adsorption trials in the presence of different concentration of RB, 2.5 mg L^{-1} and 5 mg L^{-1}, and TRGO, from 12.5 mg L^{-1} to 50 mg L^{-1} were performed, and, as expected, the percentage of adsorption increased with the amount of TRGO. However, it is interesting to note that the removal of RB *via* adsorption is almost complete, even with low material amount.

Table 1. Percentages of dyes adsorbed on the carbonaceous material (measured after 1 minute of equilibration in the dark); n.p. indicates not performed trials.

		TRGO 12.5 mg L^{-1}	**TRGO 25 mg L^{-1}**	**TRGO 50 mg L^{-1}**	**GOx 50 mg L^{-1}**
RB	**2.5 mg L^{-1}**	70 %	90 %	95 %	n.p.
	5 mg L^{-1}	40 %	80 %	90 %	10 %
OII	**5 mg L^{-1}**	n.p.	60 %	n.p.	n.p.
	20 mg L^{-1}	10 %	n.p.	60 %	20 %
RB + OII	**RB: 5 mg L^{-1}**	n.p.	n.p.	80 %	5 %
	OII: 20 mg L^{-1}			40 %	0 %

In the case of OII adsorption on the carbonaceous material rapidly occurred as well, but it was lower than RB; for example, in the presence of 50 mg L^{-1} TRGO almost 60% of 20 mg L^{-1} OII was removed within 1 minute. It has to be noted that adsorption on TRGO is still an important mechanism for dyes removal, also in the presence of a mixture of the two dyes (Table 1). Conversely, in the case of GOx (50 mg L^{-1}), adsorption is limited to almost 10%-20% for both dyes

and it decreased in the presence of the dyes mixture. These data are not surprisingly; TRGO seems to play a key role in dyes removal *via* adsorption mechanism due to its high surface area, while with GOx despite its high surface area, adsorption capacity is strongly linked to the presence of surficial negatively charged groups, that are able to promote the adsorption of cationic pollutants [20, 22], but in our case exerted a detrimental effect. In fact, OII in our experimental conditions (pH=6) is negatively charged, so prevailing the repulsion effect and therefore adsorption is hindered. RB, even if contains a cationic group, also possess a carboxylic group (pKa=3.1) that compete with adsorption process and induce repulsion, so justifying the reduced amount of removal *via* adsorption [21, 27].

After use, TRGO can be recovered from aqueous solution by filtration and reused; the adsorption and recovery processes are illustrated in Figure 4. After the dye transfer from water to TRGO the suspension was filtered through a cellulose acetate 0.45 μm pore diameters filter and, afterwards, the adsorbed dye can be removed from the filter by ethanol extraction; the re-suspended TRGO exhibited a similar percentage of removal by adsorption as pristine material.

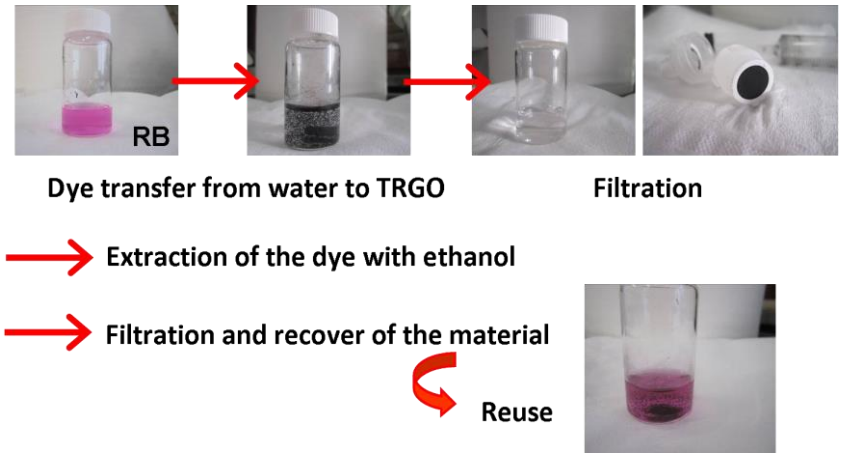

Figure 4. Illustration of RB (5 mg L^{-1}) adsorption on TRGO (50 mg L^{-1}) and the recovery of the carbonaceous adsorbent material for reuse in a new dye-treatment.

The results reported hereafter concern trials performed fixing the concentration of RB at 5 mg L^{-1} and the concentration of OII at 20 mg L^{-1}.

In Figures 5 the disappearance curves for RB (a) and OII (b) in the presence of GOx (50 mg L^{-1}) or TRGO (50 mg L^{-1}) as a function of the treatment time are shown; for comparison purpose in Figure 5a also the curve concerning the adsorption in the dark of RB on TRGO is reported. The y-axis shows the ratio between the absorbance at a certain time and the absorbance at time zero; the Abs/Abs_0 at time zero corresponds to 100% of the initial dye concentration in the case of direct

photolysis, whereas in the other cases matches with the fraction not adsorbed on the carbonaceous material, i.e. 10% for the RB with TRGO, about 90% for the RB with GOx, 40% for the OII with TRGO and about 80% for the OII with GOx (see data collected in Table 1).

Direct photolysis was limited for OII within the treatment time considered (below 20% after 6 hours), whereas it contributed to RB degradation and almost 50% was abated in the considered time.

Following the addition of CNPs, RB in the presence of TRGO is chiefly (and instantly, approximately 1 min) removed by adsorption; the remaining amount (almost 10%, 0.5 mg L^{-1}) could be eliminated *via* adsorption in the dark within 30 min or *via* adsorption/degradation under visible light in 15 min. This slight difference could be ascribed to a direct photolysis process contribution rather than to a photoinduced process mediated by TRGO, as due its almost zero band-gap TRGO is known to be unable to induce a degradation. As expected, OII is initially partially adsorbed on TRGO (60%), but no further adsorption occurs in the dark or in the dark/light; since direct photolysis is limited, no photo-contribution to the OII degradation is involved in the considered time. Therefore, considering the similarity between the dark adsorption and the irradiation curve, only the second one is reported in Figure 5b.

In addition, it has to be underlined that the presence of TRGO reduces the effect of the direct photolysis on both molecules; this behavior is probably due to the darkening effect of TRGO that restricted the light penetration in the aqueous solution.

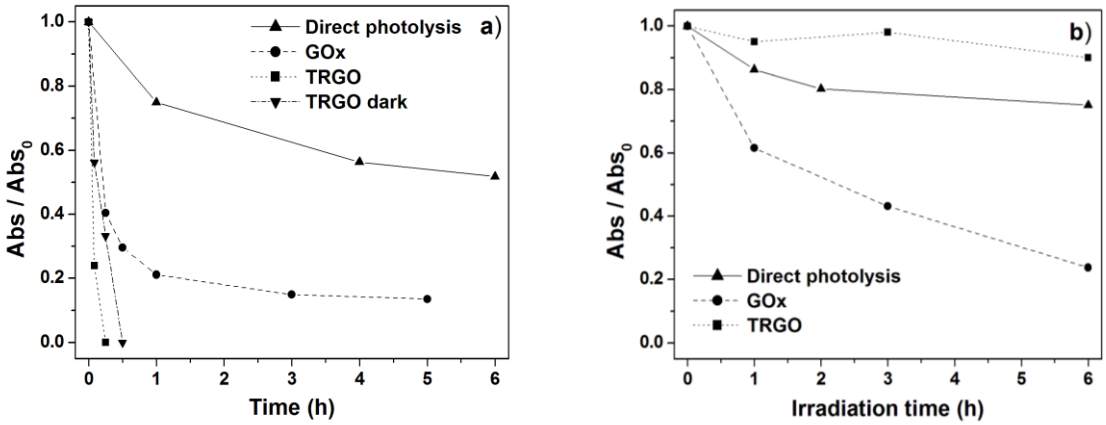

Figure 5. RB (initial concentration 5 mg L^{-1}, a) and OII (initial concentration 20 mg L^{-1}, b) disappearance curves as a function of time. Direct photolysis (▲), 50 mg L^{-1} TRGO dark adsorption profile (▼), irradiations performed in the presence of 50 mg L^{-1} TRGO (■) and GOx (●).

Conversely, GOx is able to induce dyes photodegradation and almost 80% of the residual dyes (90 % of initial RB, and 80 % of initial OII) are abated within 5 hours of irradiation under simulated

solar light; in this system, the corresponding pseudo-first order rate constants (k) are 0.57 h^{-1} for OII and 4.01 h^{-1} for RB.

This behavior has been already assessed on the phenol degradation [14] and could be attributed to the different band-gap of the carbonaceous materials, as the band-gap of graphene derivatives can be tuned by modifying the degree of oxidation, with a change of the optical gap from 3.5 eV down to 1 eV by increasing the C/O ratio [28]; therefore, GOx shows typical band-gap of semiconductor.

We try to exploit the key peculiarities of these materials to tune the way of action of these materials by employing TRGO and GO together. A mixture of the two dyes was treated using a combination of the two materials tested employing different ratios; the best performance was achieved when GOx:TRGO ratio is close to 1 and the results are plotted in Figure 6.

The Abs/Abs_0 at time zero corresponds to the fraction not adsorbed on the carbonaceous materials, i.e. 20% for RB and 60% for OII; therefore the instantaneous adsorption also in this case was observed. The residual dyes (about 1 mg L^{-1} of RB and 12 mg L^{-1} of OII) disappearance reached 70% for RB and 40% for OII after three hours of irradiation. In this case, compare to trial on separate dyes, the corresponding pseudo-first order rate constants increase for OII (from 0.57 to 2.14 h^{-1}) and decrease for RB (from and 4.01 to 2.67 h^{-1}). These results show that a mixture of TRGO and GOx allowed the exploitation of the adsorbent and the photosensitizer properties of the two materials to obtain dyes removal.

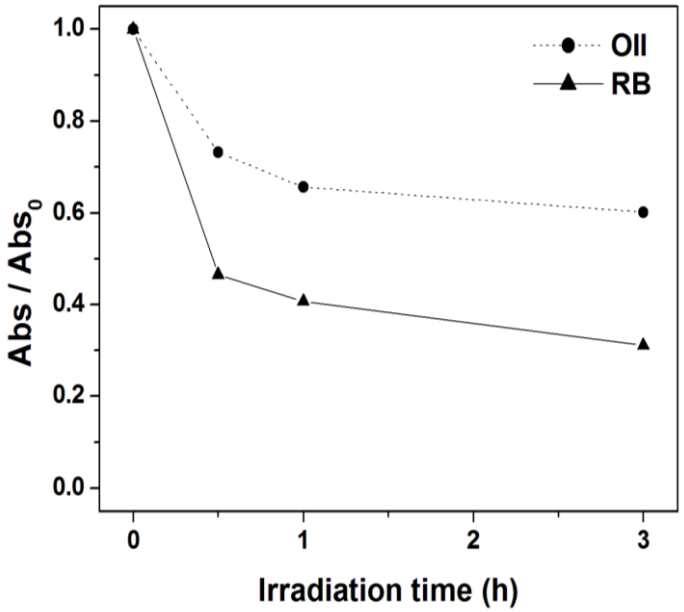

Figure 6. RB (initial concentration 5 mg L^{-1}, ▲) and OII (initial concentration 20 mg L^{-1}, ●) disappearance curves as a function of irradiation time. The two dyes were irradiated in mixture in the presence of GOx (50 mg L^{-1}) and TRGO (50 mg L^{-1}).

3.2. Carbonaceous materials dispersed in PEGDA crosslinked films

The possibility to have the material in film form rather than powder dispersion into aqueous solution allows a reduction of the costs of disposal and recovery of the material at the end of the process.

For this reason, the second step of this investigation involved the dispersion of GOx and/or TRGO into an UV-curable acrylic resin and the crosslinked films were investigated in the dyes removal from water.

The addition of the carbonaceous filler in the photocurable PEGDA resin was varied in order to obtain different types of materials (see Table 2). The UV-curing process was investigated *via* RT-FTIR analysis; notwithstanding the possible shielding effect of the carbon fillers towards UV-light, the photo-curing process and final acrylic double bond conversion are not significantly affected, and it is possible to achieve fully cured films, as already reported in previous investigation [29-31].

High gel contents (above 98%, see Table 2) were measured for all the cured films, as an indication of the formation of a tight crosslinked network and the absence of extractable monomers or oligomers in the cured system. Differential scanning calorimetry (DSC) was performed on cured films in order to evaluate the glass transition temperature (Tg, Table 2). It is possible to observe an increase of Tg by increasing the filler content into the UV-curable formulations, in accordance with the previous data reported in literature [30], and attributable to an hindering of the mobility of the PEGDA network by the carbonaceous filler with a consequent increase of Tg. Nevertheless, the crosslinked PEGDA films maintained its elastomeric behavior with a Tg values much below room temperature also in the presence of the fillers.

Table 2. Properties of PEGDA based UV-curing films.

Sample	Conversion (%)[1]	Gel Content (%)[2]	Tg (°C)[3]
PEGDA	98	100	-60
PEGDA + 1 wt% GOx	98	99	-55
PEGDA + 1 wt% TRGO	93	99	-55

[1] Determined *via* FT-IR following the decrease of the acrylic double bond peak centered at 1640 cm^{-1}. Radical photoinitiator concentration 2 wt%. Light intensity 30 mW/cm^2. Film thickness 50 μm.
[2] Measured after 24 hours extraction in chloroform, ASTM D2765-84.
[3] Measured by DSC on crosslinked films. Film thickness 50 μm.

The efficiency of the crosslinked films in dyes removal either *via* adsorption or photodegradation was evaluated on OII and/or RB. A blank experiment was performed as well with the pristine acrylic film, evidencing a negligible dyes disappearance.

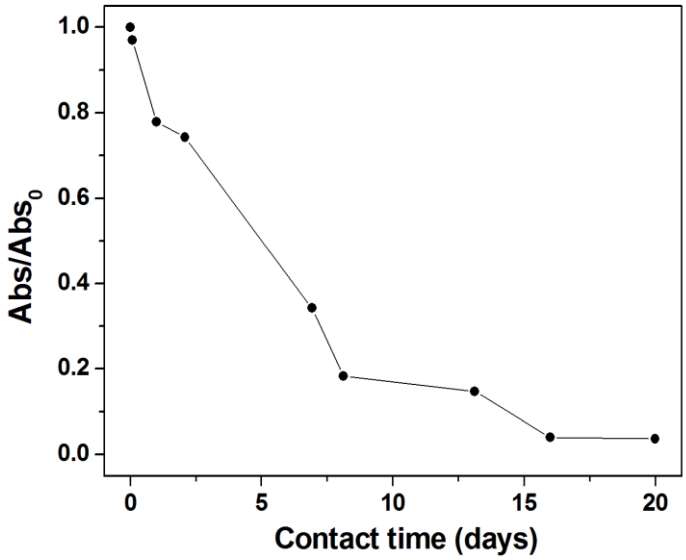

Figure 7. RB (5 mg L^{-1}) adsorption profile as a function of contact time with PEGDA UV-cured films containing 1 wt% TRGO.

Differently from what occurring with materials dispersed in aqueous solution, the kinetic of adsorption in the dark in the presence PEGDA UV-cured film containing 1 wt% TRGO becomes very slow and RB removal *via* adsorption is achieved only after very long time (20 days), as perceived by Figure 7. This result was expected, as the dispersion of TRGO within the polymeric films caused a reduction of the exposed superficial area.

Preliminary experiments were performed in the presence of films filled with different amount of CNPs and efficiency was maxima with 1 wt% of CNPs. RB and OII disappearance curves obtained under solar light irradiation in the presence of films containing 1 wt% GOx or a mixture of 1 wt% GOx and 1 wt% TRGO are reported in Figures 8; for comparison purpose, also the adsorption profiles in the presence of film containing 1 wt% TRGO are shown. As already reported in Figure 5 for RB, the adsorption on TRGO within 24 hours is negligible; therefore, the Abs/Abs_0 at time zero plotted in Figure 5 corresponds to 100% of the initial dye concentration. Irradiation experiments in the presence of TRGO films were not performed, due to the already discussed zero band-gap.

When employing 1 wt% of GOx film, complete bleaching was achieved within about 22 hours of irradiation for both RB and OII. When both CNPs are dispersed into a polymeric matrix, the removal of the dye can only be achieved *via* photodegradation. The constant rate are lowered to

0.24 and 0.12 h^{-1} for RB and OII, respectively. It has to be noted that not only the synergistic effect observed when dispersed in water was lost, but the combined addition of GOx/TRGO within the film exhibits a detrimental effect, reasonably attributable to a darkening effect exerted by TRGO.

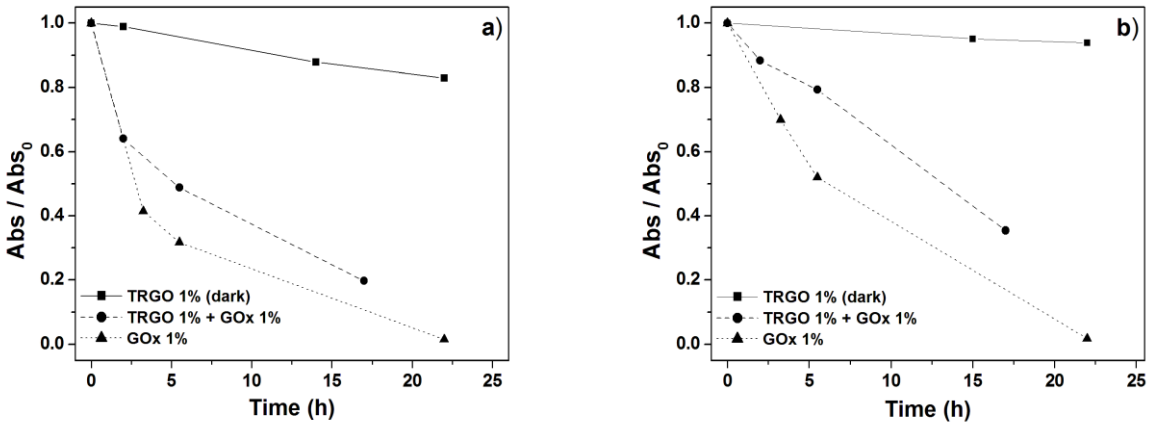

Figure 8. RB (5 mg L^{-1}, a) and OII (20 mg L^{-1}, b) disappearance curves as a function of time. Adsorption profile in the dark in the presence of PEGDA UV-cured films containing 1 wt% TRGO (■) and photobleaching profiles in the presence of films containing 1 wt% GOx (▲) and 1 wt% GOx + 1 wt% TRGO (●).

4. CONCLUSIONS

In this paper we report the use of graphite oxide (GOx) and/or thermally reduced graphite oxide (TRGO) for the removal of dyes from water. We exploited the key peculiarities of the photoactivity of GOx and the high adsorption capability of TRGO. We demonstrated that TRGO acts as a good adsorbent material when dispersed in aqueous solution whereas GOx can be used as an efficient photosensitizer.

Dye removal is almost complete in the dark in the presence of TRGO and within few minutes a steady-state concentration was achieved, with a higher efficiency in Rhodamine B (RB) removal with respect to Orange II (OII). Similar results were also obtained in the presence of a mixture of the two dyes showing that TRGO plays a key role in dyes removal *via* adsorption mechanism due to its high surface area.

On the contrary, in the case of GOx, adsorption is limited to almost 10%-20% for both dyes, but this material is able to induce efficient dyes photodegradation and almost 80% of the residual dyes (90 % of initial RB, and 80 % of initial OII) are abated within 5 hours of irradiation under simulated solar light. It has also to underlined that the irradiation experiments were performed with simulated

solar light; GOx could be used to improve the degradation of RB, which already was degraded by direct photolysis, and to promote the OII abatement, exploiting the solar radiation, the cheapest and environmental friendly energy resource.

Furthermore we present here, for the first time, the possibility to use these carbon nanoparticles (CNPs) not only dispersed in aqueous solution but also within an UV-cured polymeric coating.

The UV-curing process was investigated when the CNPs were added in the UV-curable acrylic resin, the crosslinked films were fully characterized and the efficiency in dyes removal either *via* adsorption or photodegradation was evaluated. When the graphene derivatives were dispersed in UV-cured acrylic polymeric films, the reduction of the surface area dropped the adsorption properties of TRGO, whereas the photosensitizer properties of GOx were maintained and the bleaching of the two dyes was achieved.

Acknowledgements

We acknowledge support from a Marie Curie International Research Staff Exchange Scheme Fellowship (PHOTOMAT, proposal no. 318899) within the 7th European Community Framework Programme.

References

[1] M. Sökmen, A. Özkan, Decolourising textile wastewater with modified titania: the effects of inorganic anions on the photocatalysis, J. Photochem. Photobiol. A 147 (2002) 77-81.

[2] C. Hachem, F. Bocquillon, O. Zahraa, M. Bouchy, Decolourization of textile industry wastewater by the photocatalytic degradation process, Dyes Pigment 49 (2001) 117–125.

[3] I. Arslan, I.A. Balcioglu, D.W. Bahnemann, Advanced chemical oxidation of reactive dyes in simulated dyehouse effluents by ferrioxalate-Fenton/UV-A and TiO(2)/UV-A processes, Dyes Pigment 47 (2000) 207–218.

[4] K. Rajeshwar, M.E. Osugi, W. Chanmanee, C.R. Chenthamarakshan, M.V.B. Zanoni, P. Kajitvichyanukul, R. Krishnan-Ayer, Heterogeneous photocatalytic treatment of organic dyes in air and aqueous media, J. Photochem. Photobiol. C 9 (2008) 171–192.

[5] Y.M. Xu, C.H. Langford, UV- or visible-light-induced degradation of X3B on TiO(2) nanoparticles: The influence of adsorption, Langmuir 17 (2001) 897–902.

[6] M. Vautier, C. Guillard, J.M. Hermann, Photocatalytic degradation of dyes in water: Case study of indigo and of indigo carmine, J. Catal. 201 (2001) 46–59.

[7] D. Fabbri, P. Calza, A. Bianco Prevot, Photoinduced transformations of Acid Violet 7 and Acid Green 25 in the presence of TiO_2 suspension, J. Photochem. Photobiol. A 213 (2010) 14–22.

[8] G.A. Epling, C. Lin, Photoassisted bleaching of dyes utilizing TiO_2 and visible light, Chemosphere 46 (2002) 561–570.

[9] M.C. Long, Y. Qin, C. Chen, X.Y. Guo, B.H. Tan, W.M. Cai, Origin of Visible Light Photoactivity of Reduced Graphene Oxide/TiO_2 by in Situ Hydrothermal Growth of Undergrown TiO_2 with Graphene Oxide, J. Phys. Chem. C 117 (2013) 16734–16741.

[10] V. Stengl, D. Popelkova, P. Vlacil, TiO_2-Graphene Nanocomposite as High Performace Photocatalysts, J. Phys. Chem. C 115 (2011) 25209–25218.

[11] J. Du, X.Y. Lai, N.L. Yang, J. Zhai, D. Kisailus, F.B. Su, D. Wang, L. Jiang, Hierarchically Ordered Macro-Mesoporous TiO_2-Graphene Composite Films: Improved Mass Transfer, Reduced Charge Recombination, and Their Enhanced Photocatalytic Activities, ACS Nano 5 (2011) 590-596.

[12] B.J. Jiang, C.G. Tian, W. Zhou, J.Q. Wang, Y. Xie, Q.J. Pan, Z.Y. Ren, Y.Z .Dong, D. Fu, J.L. Han, H.G. Fu, In Situ Growth of TiO_2 in Interlayers of Expanded Graphite for the Fabrication of TiO_2-Graphene with Enhanced Photocatalytic Activity, Chem-Eur. J. 17 (2011) 8379–8387.

[13] M. Sangermano, P. Calza, M.A. Lopez-Manchado, Graphene oxide-epoxy hybrid material as innovative photocatalyst, J. Mater. Sci. 48 (2013) 5204-5208.

[14] M. Minella, M. Demontis, M. Sarro, F. Sordello, P. Calza, C. Minero Photochemical stability and reactivity of Graphene Oxide, J. Mater. Sci. 50 (2015) 2399-2409.

[15] W. Chean, S. Hosseini, M.A. Khan, T.G. Chuah, T.S.Y. Choong, Acid modified carbon coated monolith for methyl orange adsorption, Chem. Eng. J. 215 (2013) 747-754.

[16] V. Vimonses, S.M. Lei, B. Jin, C.W.K. Chow, C. Saint Adsorption of congo red by three Australian kaolins, Appl. Clay Sci. 43 (2009) 465-472.

[17] A.V. Rao, N.D. Hegde, H. Hirashima, Absorption and desorption of organic liquids in elastic superhydrophobic silica aerogels, J. Colloid Interf. Sci. 305 (2007) 124-132.

[18] R.A.A. Muzzarelli, J. Boudrant, D. Meyer, N. Manno, M. DeMarchis, M.G. Paoletti, Current views on fungal chitin/chitosan, human chitinases, food preservation, glucans, pectins and inulin: A tribute to Henri Braconnot, precursor of the carbohydrate polymers science, on the chitin bicentennial, Carbohyd. Polym 87 (2012) 995-1012.

[19] H. Chen, Gao B, H. Li, Removal of sulfamethoxazole and ciprofloxacin from aqueous solutions by graphene oxide, J. Hazard. Mater. 282 (2015) 201-207.

[20] P. Sharma, B.K. Saikia, M.R. Das, Removal of methyl green dye molecule from aqueous system using reduced graphene oxide as an efficient adsorbent: Kinetics, isotherm and thermodynamic parameters, Colloids and Surfaces A: Physicochem. Eng. Aspects 457 (2014) 125–133.

[21] M. Yusuf, F. M. Elfghi, S. Abbas Zaidi, E.C. Abdullahab, M. Ali Khan, Applications of graphene and its derivatives as an adsorbent for heavy metal and dye removal: a systematic and comprehensive overview, RSC Adv. 5 (2015) 50392–50420.

[22] P. Bradder, S. King Ling, S. Wang, S. Liu, Dye Adsorption on Layered Graphite Oxide, J. Chem. Eng. Data 56 (2011) 138–141.

[23] H.C. Schniepp, J.L. Li, M.J. McAllister, H. Sai, M. Herrera-Alonso, D.H. Adamson, R.K. Prud'homme, R. Car, D.A. Saville, I.A. Aksay, Functionalized single graphene sheets derived from splitting graphite oxide, J. Phys. Chem. B 110 (2006) 8535-8539.

[24] R. Verdejo, F. Barroso Bujans, M.A. Rodriguez-Perez, J.A. de Saja, M.A. Lopez Manchado, Functionalized graphene sheet filled silicone foam nanocomposites, J. Mater. Chem. 18 (2008) 2221-2226.

[25] S. Bittolo Bon, L. Valentini, R. Verdejo, J.L. Garcia Fierro, L. Peponi, M.A. Lopez-Manchado, J.M. Kenny, Plasma fluorination of chemically derived graphene sheets and subsequent modification with butylamine, Chem. Mater. 21(2009) 3433-3438.

[26] K.N. Kudin, B. Ozbas, H.C. Schniepp, R.K. Prud'homme, I.A. Aksay, R. Car, Raman Spectra of Graphite Oxide and Functionalized Graphene Sheets, Nano Letters 8 (2007) 36-41.

[27] K. Shen, M.A. Gondal, Removal of hazardous Rhodamine dye from water by adsorption onto exhausted coffee ground, J. Saudi Chem. Soc. (2013), in press.

[28] A. Mathkar, D. Tozier, P. Cox, P.J. Ong, C. Galande, K. Balakrishnan, A.L.M. Reddy, P.M. Ajayan, Controlled, Stepwise Reduction and Band Gap Manipulation of Graphene Oxide, J. Phys. Chem. Lett. 3 (2012) 986-991.

[29] M. Martin-Gallego, R. Verdejo, M.A. Lopez-Manchado, M. Sangermano, Epoxy-Graphene UV-cured nanocomposites, Polymer 52 (2011) 4664-4669.

[30] M. Sangermano, S. Marchi, L. Valentini, S.B. Bon, P. Fabbri, Transparent and Conductive Graphene Oxide/Poly(ethylene glycol) diacrylate Coatings Obtained by Photopolymerization, Macromol. Mater. Eng. 296 (2011) 401-407.

[31] P. Fabbri, L. Valentini, S.B. Bon, D. Foix, L. Pasquali, M. Montecchi, M. Sangermano, In-situ graphene oxide reduction during UV-photopolymerization of graphene oxide/acrylic resins mixtures, Polymer 53 (2012) 6039-6044.